JOURNAL OF SOLID STATE CHEMISTRY 37, 308–317 (1981)

Neutron Powder Diffraction and Magnetic Measurements on $RbTiI_3$, $RbVI_3$, and $CsVI_3$

H. W. ZANDBERGEN

Gorlaeus Laboratories, University of Leiden, P.O. Box 9502, 2300 RA Leiden, The Netherlands

Received June 18, 1980; revised form September 10, 1980

$CsVI_3$ (a = 8.124(1) c = 6.774(1) Å, Z = 2, $P6_3/mmc$ at 293 K) adopts the $BaNiO_3$ structure. Three-dimensional magnetic ordering takes place at T_c = 32(1) K. At 1.2 K the magnetic moment is 1.64(5) μ_B and it forms a 120° spin structure in the basal plane. $RbVI_3$ (a = 13.863(2) c = 6.807(1) Å, Z = 6, $P6_3cm$ *or* $P\bar{3}c1$ at 293 K) and $RbTiI_3$ (a = 14.024(3) Å, c = 6.796(2) Å, Z = 6, $P6_3cm$ or $P\bar{3}c1$ at 293 K) adopt a distorted $BaNiO_3$ structure, probably isostructural with $KNiCl_3$. T_c of $RbVI_3$ is 25(1) K. At 1.2 K, $RbVI_3$ has a spin structure similar to the one of $CsVI_3$ with a magnetic moment of 1.44(6) μ_B. $RbTiI_3$ shows no magnetic ordering at 4.2 K. It is shown that a deviation from the 120° structure is expected for compounds with a distorted $BaNiO_3$ structure such as $RbVI_3$. The cell dimensions of $CsTiI_3$ are reported.

Introduction

The investigations on the title compounds are part of our research program on the crystallographic and magnetic properties of the compounds in the series AI–BI_2, A being K, Rb, Cs, In, or Tl, and B a first-row transition element, Mg, Zn, Cd, or Hg.

Two structure types exist for the ABI_3 compounds, viz., the NH_4CdCl_3 structure ($TlMnI_3$ (*1, 2*), $TlFeI_3$ (*2*), and $TlCdI_3$ (*3*)) and the $BaNiO_3$ structure (see Table I).

The compounds with the $BaNiO_3$ structure have been studied extensively because of their quasi-one-dimensional behavior. Crystallographic and magnetic measurements are reported of the V compounds $RbVCl_3$, $CsVCl_3$, $CsVBr_3$, and $CsVI_3$ (*4–6*). These compounds exhibit very strong one-dimensional antiferromagnetic behavior. The exchange interaction of $CsVI_3$ is reported to be −61(8) K. However, a bad fit was obtained using the model of Smith and Friedberg (*5, 7*) $CsVI_3$ is reported to be isostructural to $BaNiO_3$ (*5*).

In this paper the results of neutron powder diffraction and magnetic measurements on single crystals of $RbVI_3$ and $CsVI_3$ and a powder of $RbTiI_3$ are reported.

Experimental

The title compounds were prepared from a stoichiometric mixture of the binary compounds. Ultrapure RbI and CsI purchased from Merck were used. VI_2 was prepared from the elements in an almost horizontal evacuated and sealed quartz tube in a furnace with a temperature gradient 200°C (I side)–900°C (V side). TiI_2 was prepared by disproportion of TiI_3 which was prepared in a manner similar to that used for VI_2 (200–700 °C). The preparation of pure samples is very difficult because of the high sensitivity

0022-4596/81/060308-10$02.00/0

TABLE I

CELL DIMENSIONS AT 293 K OF ABI_3 COMPOUNDS WITH A $BaNiO_3$-LIKE STRUCTURE[a]

Compound	Diffraction type	a (Å)	b (Å)	c (Å)	β (deg)
$RbTiI_3$	ND	14.024(3)		6.796(2)	
$CsTiI_3$	XD	8.205(5)		6.784(5)	
$RbVI_3$	ND	13.863(2)		6.807(1)	
$CsVI_3$	ND	8.124(1)		6.774(1)	
$RbCrI_3$	ND	13.772(2)	8.000(1)	7.069(1)	95.85(1)
$CsCrI_3$	ND	8.126(1)		6.944(1)	
$CsMnI_3$	ND	8.190(1)		6.958(1)	
$CsFeI_3$	ND	8.122(1)		6.807(1)	
$CsNiI_3$	XD	8.007(3)		6.707(4)	

[a] The cell dimensions are determined by profile refinement (*10*) of neutron powder diffraction measurements (ND) or by least-squares refinement of 2Θ values taken from X-ray diffraction diagrams (XD). The unit cell of $RbCrI_3$ is monoclinic distorted due to the cooperative Jahn–Teller effect.

to air and moisture and the possible formation of other compounds such as $A_3B_2I_9$. The samples of $CsVI_3$ and $RbVI_3$, used for neutron diffraction, were powdered and annealed several times at 750°C. $RbTiI_3$ can only be prepared by annealing below 450°C since TiI_2 disproportionates above this temperature (*8*). No pure samples could be prepared. On top of problems arising from the possible formation of Rb_2TiI_6 and $Rb_3Ti_2I_9$, the compound is so sensitive to air and moisture that although all manipulations were done in a dry glovebox under argon, samples were more contaminated after each cycle of powdering and annealing. $CsTiI_3$ could not be prepared below 450°C. When the proper amounts of CsI and TiI_2 were melted in an evacuated quartz tube for 2 min at 800°C the X-ray diffraction pattern of this sample contained reflections of Cs_2TiI_6 besides reflections of $CsTiI_3$. The cell dimensions of $CsTiI_3$ are given in Table I.

The compounds must be kept in evacuated sealed glass tubes. Compounds kept in a tube with nitrogen or argon and closed with a rubber stopper kept losing I_2.

Single crystals of $CsVI_3$ and $RbVI_3$ were grown using the Bridgman method. Although, after melting, a stoichiometric mixture of the binary compounds contained RbI and VI_2, suggesting $RbVI_3$ to be incongruent, it was possible to obtain by this method single crystals of $RbVI_3$ large enough for the magnetic measurements. The single crystals of $CsVI_3$ and $RbVI_3$ used for the magnetic measurements were cut from a larger single crystal. Since the crystals cleave very easily along the (1 1 0) plane the cutting of the crystals along the (0 0 1) plane had to be done very gently.

In the low-temperature region magnetic measurements were performed by means of a Vibrating Sample Magnetometer (*9*) equipped with a superconducting magnet supplying fields up to 56 kOe. In the temperature region 80–300 K the temperature dependence of the susceptibility was measured on a powder of $RbVI_3$ using the Faraday method.

Neutron powder diffraction recordings were collected of $CsVI_3$ (293 and 1.2 K), $RbVI_3$ (293 and 1.2 K), and $RbTiI_3$ (293 and 4.2 K) at the HFR reactor at Petten (The Netherlands) using $\lambda = 2.5722(2)$ Å with 30′ collimation in the angular region $4° < 2\theta < 139°$. The recording of $RbTiI_3$ at 4.2 K was done in the angular region $4° < 2\theta < 90°$ with a higher counting time in order to obtain higher resolution.

The profile program of Rietveld (*10*) was used for the refinements. No absorption corrections were applied. The coherent scattering lengths used (*11*) are $b(\mathrm{Rb}) = 0.71$, $b(\mathrm{Cs}) = 0.55$, $b(\mathrm{Ti}) = -0.34$, $b(\mathrm{V}) = -0.038$, and $b(\mathrm{I}) = 0.53$, all in units of 10^{-12} cm. The magnetic form factors were taken from Watson and Freeman (*12*).

Refinements on the Neutron Diffraction Data

$CsVI_3$ 293 K

The refinement in space group $P6_3/mmc$

was started with the positions of the ions in $CsMnI_3$ (*11*), which adopts the $BaNiO_3$ structure. Full matrix refinement led to convergence at

$$R(\text{total}) = \sum_i \Big| I_i(\text{obs}) - (1/c) I_i(\text{calc}) \Big| \Big/ \sum_i I_i(\text{obs}) = 0.044$$

and

$$R(\text{profile}) = \Big\{ \sum_j w_j (y_j(\text{obs}) - (1/c) y_j(\text{calc}))^2 \Big/ \sum_j w_j (y_j(\text{obs}))^2 \Big\}^{1/2} = 0.128,$$

where I_i is the intensity of the ith reflexion and y_j is the intensity of the jth measuring point; w_j is a statistical weight factor and c is a scaling factor. Refinements in the space groups $P6_3mc$ and $P\bar{6}2c$ did not lead to significantly lower R values and shifts of the ions. The observed and calculated profiles are shown in Fig. 1. The final

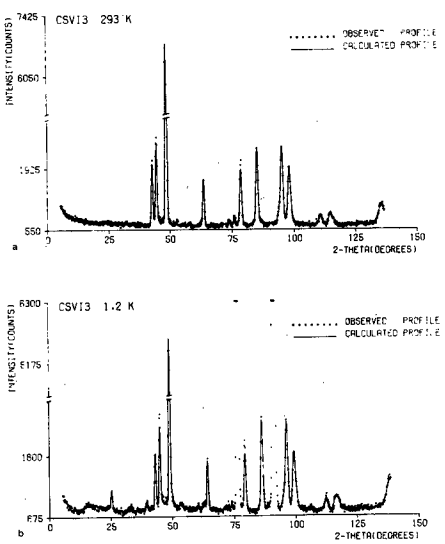

FIG. 1. The observed and calculated diffraction profiles of $CsVI_3$ at (a) 293 and (b) 1.2 K. The large peaks at 77 and 91° are due to the cryostate.

TABLE II

CELL DIMENSIONS, POSITIONAL PARAMETERS, OVERALL ISOTROPIC THERMAL PARAMETER ($b_0 = 8(\pi\bar{U})^2$ Å^2 (*17*)), AND THE MAGNETIC MOMENT OF $CsVI_3$ WITH A 120° STRUCTURE IN THE BASAL PLANE

293 K

a = 8.124(1) Å c = 6.774(1) Å b_0 = 2.9(1) Å^2

	x	y	z	μ (μ_B)
Cs	$\frac{1}{3}$	$\frac{2}{3}$	$\frac{1}{4}$	
V	0	0	0	
I	0.169(1)	−0.169(1)	$\frac{1}{4}$	

1.2K

a = 8.062(1) Å c = 6.704(1) Å b_0 = 0.1(1) Å^2

Cs	$\frac{1}{3}$	$\frac{2}{3}$	$\frac{1}{4}$	
V	0	0	0	1.64(5)
I	0.1734(6)	−0.1734(6)	$\frac{1}{4}$	

parameters and some relevant distances and bond angles are listed in Table II and III.

$CsVI_3$ 1.2 K

The diffraction diagram of $CsVI_3$ recorded at 1.2 K contains a number of extra weak reflections. These reflections must originate in a three-dimensional magnetic ordering since the intensities of the reflections decrease rapidly with increasing 2θ. The extra reflections can all be indexed to an $a3^{1/2}$, $a3^{1/2}$, c unit cell, a and c being the axes of the nuclear unit cell.

Four magnetic models were introduced in the refinement, viz., two collinear and two 120° structures (see Fig. 2). Of these four models the 120° structure with the tion pattern that $CsVI_3$ adopts a distorted $BaNiO_3$ structure like $RbVI_3$ does.

TABLE III

SOME DISTANCES (Å) AND BOND ANGLES (°) IN $CsVI_3$ AT 293 K

Cs–I	4.10(1)	I–I	4.00(1)
Cs–I	4.06(1)	I–I	4.12(1)
V–I	2.92(1)	I–I	4.14(1)
V–I–V	70.8(4)		

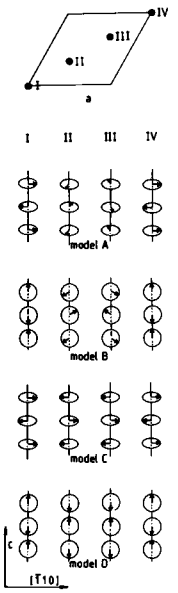

FIG. 2. The magnetic structures used as models for the refinements. The magnetic unit cell with the chains I–IV is given in a. Model A and B are 120° structures in the basal plane and (1 1 0) plane, respectively. In model C and D the magnetic moments are parallel to [1 1 0] and [0 0 1], respectively.

magnetic moments in the basal plane resulted in the lowest R value for the magnetic intensity part of R(total) (see Table IV).

No indication was found from the diffrac-

TABLE IV

THE FINAL R VALUES OF THE REFINEMENTS OF $CsVI_3$ AND $RbVI_3$ AT 1.2 K

	R(profile)	R(total)	R(nuclear)	R(magnetic)
$CsVI_3$ $P6_3/mmc$				
Model A	0.139	0.070	0.061	0.199
Model B	0.141	0.073	0.061	0.250
Model C	0.139	0.070	0.061	0.202
Model D	0.152	0.081	0.061	0.416
$RbVI_3$ $P6_3cm$				
Model A	0.162	0.123	0.121	0.197
Model B	0.166	0.128	0.121	0.322
Model C	0.166	0.128	0.121	0.306
Model D	0.173	0.133	0.120	0.456
$RbVI_3$ $P\bar{3}c1$				
Model A	0.169	0.125	0.123	0.202
Model B	0.175	0.130	0.124	0.310
Model C	0.170	0.126	0.122	0.234
Model D	0.170	0.136	0.126	0.432

The final parameters for the magnetic model with a 120° spin arrangement in the basal plane are given in Table II and the observed and calculated profiles are depicted in Fig. 1.

$RbVI_3$ 293 K

Zero- and upper-level Weissenberg photographs taken at 293 K show $RbVI_3$ to have a unit cell which can be described as an $a3^{1/2}$, $a3^{1/2}$, c superstructure of the $BaNiO_3$ structure. The zero-level (h k 0) photograph contained no superreflections. The deviation from the $BaNiO_3$ structure must be found mainly in a shift of the BX_3 chains along the c axis because of the absence of {h k 0} superreflections. Since the mirror plane perpendicular to the c axis is destroyed by these shifts the space groups $P6_3/mcm$ and $P\bar{6}c2$ can be eliminated. Assuming that the distortion from the $BaNiO_3$ structure occurs mainly as a shift of complete BI_3 chains with a deformation of the chains as small as possible, two space groups remain to be investigated, viz., $P6_3cm$ and $P\bar{3}c1$. For both space groups one chain is fixed while the other two chains in the unit cell are shifted in the same direction for $P6_3cm$ and in opposite directions for $P\bar{3}c1$ (see Fig. 3).

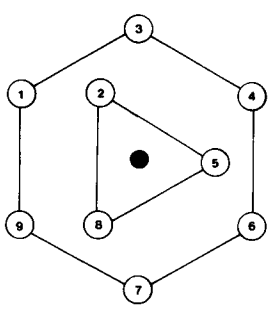

FIG. 3. A (0 0 1) projection of the coordination polyhedron of Rb^+ in $RbVI_3$. The I^- ions 1, 2, and 3 are fixed. In $P6_3cm$ the other I^- ions are shifted along the c axis in the same direction. In $P\bar{3}c1$ the shift of the ions 4, 5, and 6 is opposite to the shift of the I^- ions 7, 8, and 9.

Full matrix refinement was done for both space groups and resulted in R(profile) = 0.130 and R(total) = 0.086 for space group $P6_3cm$, and R(profile) = 0.130 and R(total) = 0.085 for space group $P\bar{3}c1$. Since the two models can not be discriminated using the R values the results of both refinements are given in Table V. The experimental and calculated profiles (for space group $P6_3cm$) are depicted in Fig. 4. Some relevant distances and bond angles for both space groups are given in Table VI.

$RbVI_3$ 1.2 K

For the refinements on the diffraction data of $RbVI_3$ recorded at 1.2 K the space groups $P6_3cm$ and $P\bar{3}c1$ were used with the four magnetic models shown in Fig. 2. Similar to $CsVI_3$ the models with the magnetic moments in the basal plane, forming a 120° arrangement, yielding the lowest R values. The final R values for all four

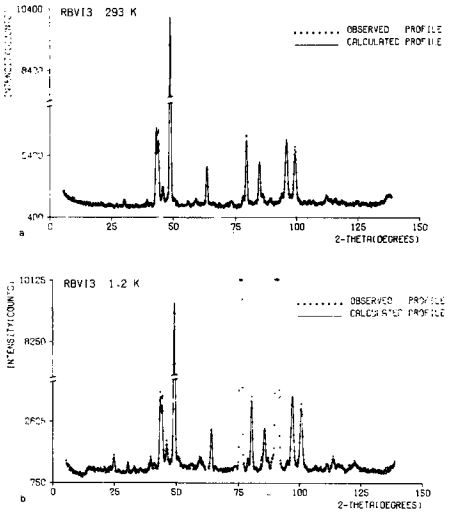

FIG. 4. The observed and calculated diffraction profiles of $RbVI_3$ at (a) 293 and (b) 1.2 K.

TABLE V

CELL DIMENSIONS, POSITIONAL PARAMETERS, OVERALL ISOTROPIC THERMAL PARAMETERS ($b_0 = 8(\pi\bar{U})^2$ Å^2 (17)) AND THE MAGNETIC MOMENT OF $RbVI_3$ WITH THE SPACE GROUPS $P6_3cm$ AND $P\bar{3}c1$ AND A MAGNETIC 120° STRUCTURE IN THE BASAL PLANE[a]

		293 K		
$P6_3cm$	a = 13.863(2) Å	c = 6.807(1) Å	b_0 = 4.5(1) Å^2	
	x	y	z	μ (μ_B)
Rb	0.330(2)	0.330(2)	0.294(5)	
V(1)	0	0	0	
V(2)	$\frac{1}{3}$	$\frac{2}{3}$	0.096(2)	
I(1)	0.166(3)	0	$\frac{1}{4}$	
I(2)	0.503(3)	0.171(2)	0.346(2)	
$P\bar{3}c1$	a = 13.863(2) Å	c = 6.807(1) Å	b_0 = 4.5(1) Å^2	
Rb	0.330(2)	0.330(2)	$\frac{1}{4}$	
V(1)	0	0	0	
V(2)	$\frac{1}{3}$	$\frac{1}{3}$	0.057(1)	
I(1)	0.169(3)	0	$\frac{1}{4}$	
I(2)	0.506(2)	0.170(1)	0.193(1)	
		1.2 K		
$P6_3cm$	a = 13750(2) Å	c = 6.761(2) Å	b = 1.5(1) Å^2	
Rb	0.333(3)	0.333(3)	0.277(4)	
V(1)	0	0	0	1.44(6)
V(2)	1.3	$\frac{2}{3}$	0.101(2)	1.44(6)
I(1)	0.161(3)	0	$\frac{1}{4}$	
I(2)	0.505(2)	0.168(3)	0.351(2)	
$P\bar{3}c1$	a = 13.750(2) Å	c = 6.761(2) Å	b_0 = 1.5(1) Å^2	
Rb	0.334(3)	0.334(3)	$\frac{1}{4}$	
V(1)	0	0	0	1.40(6)
V(2)	$\frac{1}{3}$	$\frac{2}{3}$	0.063(1)	1.40(6)
I(1)	0.161(4)	0	$\frac{1}{4}$	
I(2)	0.510(3)	0.168(2)	0.187(1)	

[a] The z parameters of V(2) and I(2) are coupled.

TABLE VI

SOME RELEVANT DISTANCES (Å) AND BOND ANGLES (°) AT 293 K FOR $RbVI_3$ WITH SPACE GROUPS $P6_3cm$ AND $P\bar{3}c1$[a]

	$P6_3cm$	$P\bar{3}c1$
$Rb–I(1)_{1,3}$	3.97(3)	3.96(3)
$Rb–I(1)_2$	3.85(4)	4.07(3)
$Rb–I(1)_2$	4.35(4)	4.07(3)
$Rb–I(2)_{4,9}$	4.01(6)	4.05(5)
$Rb–I(2)_{6,7}$	4.07(5)	4.03(4)
$Rb–I(2)_8$	4.45(4)	3.85(2)
$Rb–I(2)_8$	3.87(4)	4.49(2)
$Rb–I(2)_5$	3.87(4)	3.85(2)
$Rb–I(2)_5$	4.45(4)	4.49(2)
V(1)–I(1)	2.86(4)	2.90(4)
V(2)–I(2)	2.83(2)	2.82(2)
V(1)–I(1)–V(1)	73.0(11)	72.0(11)
V(2)–I(2)–V(2)	73.9(6)	74.3(5)

[a] The subscript numbers refer to the I^- ions depicted in Fig. 3.

models in the space groups $P6_3cm$ and $P\bar{3}c1$ are given in Table IV. The results of the refinements on this magnetic model in both space groups are listed in Table V. The observed and calculated profiles for $P6_3cm$ are shown in Fig. 4.

In the observed diffraction profile several peaks had a small shoulder. It was investigated whether these reflections could be indexed with a larger unit cell. No satisfactory results were obtained. Further investigation is necessary.

$RbTiI_3$ 293 and 4.2 K

No sample of pure $RbTiI_3$ could be prepared. The diffraction pattern contains reflections of $RbTiI_3$ and RbI as well as other peaks. The peaks could not be indexed by simple unit cell enlargments. The peaks do not coincide with strong reflections, calculated by means of the profile program of Rietveld for TiI_2, $Rb_3Ti_2I_9$, and Rb_2TiI_6 with the atomic positions of TiI_2, $Cs_3Cr_2Cl_9$, and Cs_2TiCl_6 (*12*). Because several peaks of RbI did not overlap with other peaks, the scale factor, the cell dimensions and the half-width parameters could be determined. Next, the calculated diffraction profile of RbI was subtracted from the recorded diffraction diagram.

On these corrected diffraction data the refinements were done with three models, viz., the $BaNiO_3$ structure and the two models discussed for $RbVI_3$. The best fits were obtained for the distorted $BaNiO_3$ structures with space groups $P\bar{3}c1$ and $P6_3cm$, with R(profile) = 0.215 and R(total) = 0.148. The R values are high due to the contamination. The observed and calculated profiles are shown in Fig. 5 and the final parameters are given in Table VII.

The diffraction diagram of $RbTiI_3$ recorded at 4.2 K shows no magnetic reflections, indicating the three-dimensional ordering takes place below or not far above 4.2 K.

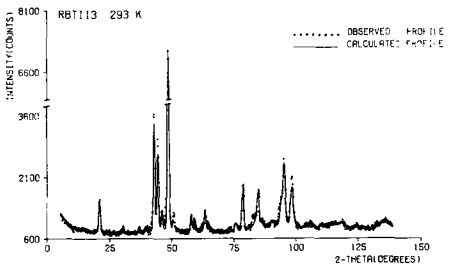

FIG. 5. The observed and calculated diffraction profiles of $RbTiI_3$ at (a) 293 K.

Magnetic Measurements

Susceptibility versus temperature and magnetization versus magnetic field measurements were performed parallel and perpendicular to the c axis on a single crystal of $CsVI_3$ (207 mg) and three equally oriented single crystals of $RbVI_3$ (total 134 mg). The magnetization vs magnetic field curves show a slight bending ($\delta M/\delta H$ is decreasing with increasing H) and contain no relevant information. The χ vs T curves depicted in Figs. 6 and 7 show a rise in χ at low temperatures due to a contamination of the crystals. The contamination is estimated to be 0.2–0.3% and must be due to a reaction of the sample with the atmosphere in the dry glovebox during the cutting of the crystals. (Very small crystals lost their transparency in a few minutes in the dry glovebox.)

TABLE VII

CELL DIMENSIONS, POSITIONAL PARAMETERS, AND OVERALL ISOTROPIC THERMAL PARAMETER ($b_0 = 8(\pi\bar{U})^2$ Å^2 (*17*)) OF $RbTiI_3$ IN SPACE GROUP $P6_3cm$ AT 293 K[a]

a = 14.024(3) Å	c = 6.796(2) Å	b_0 = 4.4(2) Å^2	
	x	y	z
Rb	0.327(3)	0.327(3)	0.280(6)
Ti(1)	0	0	0
Ti(2)	$\frac{1}{3}$	$\frac{2}{3}$	0.086(3)
I(1)	0.172(3)	0	$\frac{1}{4}$
I(2)	0.518(1)	0.166(2)	0.336(3)

[a] The z parameters of Ti(2) and I(2) are coupled.

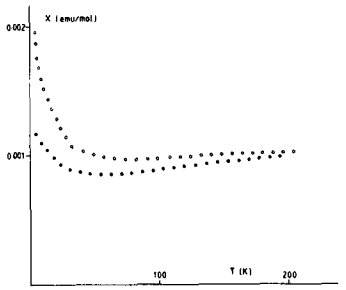

FIG. 6. The temperature dependence of the susceptibility of $CsVI_3$ parallel (open circles) and perpendicular (full circles) to the c axis, measured in a magnetic field of 9.4 kOe.

The contamination seems to make the determination of the three-dimensional transition temperature, T_c, impossible. However, considering the difference between the susceptibilities at various temperatures parallel and perpendicular to the c axis, $\chi_{\parallel c} - \chi_{\perp c}$, a sharp change is found for both compounds (see Fig. 8). A similar change is found at $T = 11$ K (see Fig. 9) for $CsMnI_3$ (*13*) which adopts a 120° structure with the magnetic moments in the (1 1 0) plane. By means of neutron diffraction and susceptibility measurements this temperature was shown to be the three-dimensional transition temperature of $CsMnI_3$. By implication the three-dimensional transition temperatures are $T_c = 32(1)$ K for $CsVI_3$ and $T_c = 25(1)$ K for $RbVI_3$.

Additionally χ vs T measurements (see Fig. 10) in the temperature region 80–330 K were done on a powder of $RbVI_3$. The

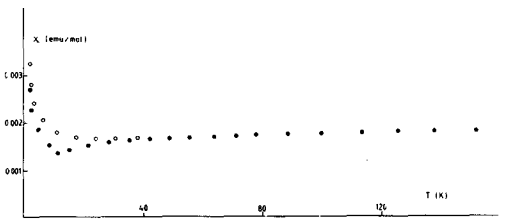

FIG. 7. The temperature dependence of the susceptibility of RbVI parallel (open circles) and perpendicular (full circles) to the c axis, measured in a magnetic field of 5.6 kOe.

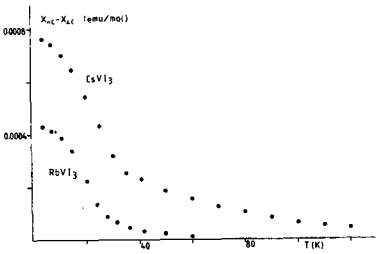

FIG. 8. $\chi_{\parallel c} - \chi_{\perp c}$ vs T for $CsVI_3$ and $RbVI_3$.

maximum in the susceptibility is found at $T = 240(10)$ K. No attempts were made to fit the observed χ vs T curve as the high-temperature region was not measured.

The χ vs T curve of $RbTiI_3$, measured on a powder, containing impurities, is shown in Fig. 11. The curve shows a very broad maximum characteristic of a one-dimensional system, with a rise at lower temperature due to paramagnetic impurities. The maximum in the susceptibility is found at 90(5) K.

Discussion

$CsVI_3$ adopts the $BaNiO_3$ structure like all $CsBI_3$ compounds do at room temperature (see Table I). $CsVI_3$ consist of face sharing VI_6 octahedra forming infinite chains in the c direction. The Cs^+ ions are in a 12 coordination of I^- ions. The ratio of the estimated ion radii (*15*) $r(Cs)/r(I)$ is 0.86. This ratio is considerably smaller for the Rb compounds: $r(Rb)/r(I) = 0.79$. The Rb^+ ion will be to small for a 12 coordina-

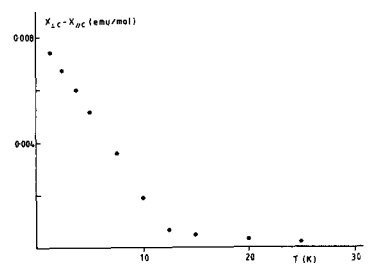

FIG. 9. $\chi_{\perp c} - \chi_{\parallel c}$ vs T for $CsMnI_3$.

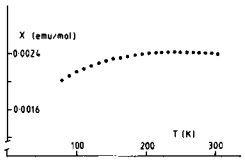

FIG. 10. Susceptibility vs temperature curve of a powder of $RbVI_3$ using the Faraday method.

tion of I^- ions and a deviation from the 12 coordination is to be expected.

As can be seen from Table VI a lower coordination for the Rb^+ ion can be realized easily by a shift of the chains along the c direction. The coordination is in first approximation 9 for space $P6_3cm$ and 10 for $P\bar{3}c1$. For comparison the Rb–I distances determined from a refinement with the $BaNiO_3$ structure as model are 4.11(1) Å (hexagon (see Fig. 2)) and 4.00(1) Å (prism).

The large isotropic thermal parameters of $RbVI_3$ and $RbTiI_3$ point to disorder. Disorder is expected because in cooling through the phase transition domains will occur, leading to stacking faults at the boundaries. Furthermore, since almost the same coordination of the Rb^+ ion is obtained for a shift in the positive or negative c direction, disorder can easily occur. Disorder is also reported for $KNiCl_3$ (*16*), which has a distorted $BaNiO_3$ structure with space group $P6_3cm$. $RbVI_3$ and $RbTiI_3$ are possibly isostructural with $KNiCl_3$.

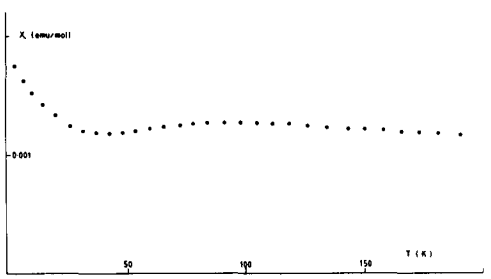

FIG. 11. Susceptibility vs temperature curve of a powder of $RbTiI_3$ measured in a magnetic field of 8.4 kOe.

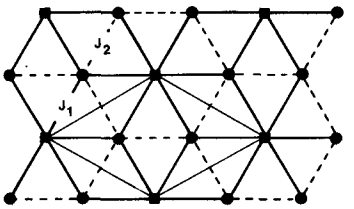

FIG. 12. A (0 0 1) plane with V^{2+} ions. The squares represent the V^{2+} ions at the origin. Two types of interchain exchange interactions, J_1 and J_2, occur, indicated by full-drawn and dashed lines, respectively. The unit is represented by the thin full-drawn lines.

The best fits to the experimental neutron diffraction data at 1.2 K were obtained for $CsVI_3$ and $RbVI_3$ with a 120° structure with the magnetic moments in the basal plane. When the in-plane anisotropy is small such a magnetic structure is to be expected for compounds with the $BaNiO_3$ structure, where the exchange interactions between a chain and its six neighboring chains are all equal. In $RbVI_3$ and $RbTiI_3$ however two types of interchain interactions, J_1 and J_2 occur as indicated in Fig. 12. When J_1 differs from J_2, which is to be expected since the exchange paths are not the same, a deviation from the 120° structure will occur. In Fig. 13 the situation for $J_1 > J_2$ is depicted. The angle, α, describing the deviation from the 120° structure, depends on the ratio J_1/J_2. Because the intensities of the magnetic reflexions of $RbVI_3$ are small no attempt was made to determine α.

Magnetic measurements on single crystals of $CsVI_3$ and $RbVI_3$ show $\chi_{\parallel c}$ to be larger than $\chi_{\perp c}$, which is consistent with the

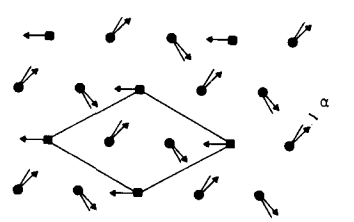

FIG. 13. A (0 0 1) plane, similar to Fig. 12, with the deviation from the 120° structure, determined by the ratio of J_1 and J_2. α is the angle of deviation.

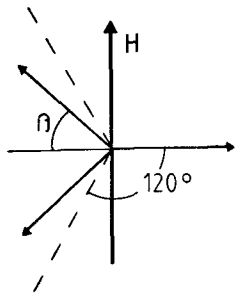

FIG. 14. The orientation in a magnetic field of the magnetic moments of a distorted 120° spin structure.

neutron diffraction results. The magnetic lattices of $CsVI_3$ and $RbVI_3$ can be divided into six sublattices, each with a sublattice magnetization $\mathbf{M}_i$ ($i = 1,6$). The antiparallel pairs of $\mathbf{M}_i$ are taken to be $\mathbf{M}_1$ and $\mathbf{M}_2$, $\mathbf{M}_3$ and $\mathbf{M}_4$, and $\mathbf{M}_5$ and $\mathbf{M}_6$. The axis $\mathbf{M}_1$–$\mathbf{M}_2$ is denoted as $\mathbf{\Delta}_1$; $\mathbf{\Delta}_2$ and $\mathbf{\Delta}_3$ for the other pairs of $\mathbf{M}_i$. The measured $\chi_{\parallel c}$ and $\chi_{\perp c}$ are to be regarded as the sum of the susceptibilities of the six sublattices. Assuming the parallel susceptibilities ($\chi_\parallel^s$) as well as the perpendicular susceptibilities ($\chi_\perp^s$) of the three pairs of sublattices to be equal, the resulting susceptibility is given by

$$\chi = \sum_{i=1}^{3} (\chi_\parallel^s \cos^2 \varphi_i + \chi_\perp^s \sin^2 \varphi_i),$$

where φ_i is the angle between $\mathbf{\Delta}_i$ and the magnetic field applied.

In the case of a 120° structure with the magnetic moments in the basal plane the total susceptibility parallel to the c axis will be

$$\chi_{\parallel c} = 3\chi_\perp^s$$

The susceptibility perpendicular to the c axis will be

$$\chi_{\perp c} = 1.5\,\chi_\parallel^s + 1.5\,\chi_\perp^s$$

With $\chi_\parallel^s$ vanishing at $T = 0$ K the expected ratio $\chi_{\parallel c}/\chi_{\perp c}$ is 2 at 0 K.

For a 120° structure the component of the energy

$$\sum_i (\chi_\parallel^s \cos^2 \varphi_i + \chi_\perp^s \sin^2 \varphi_i)H^2$$

with **H** in the basal plane is independent on the angle of **H** with an arbitrary direction in the basal plane.

However, for compounds as $RbVI_3$ with a deviation from the 120° structure the situation as depicted in Fig. 14 has the lowest energy. For this situation the ratio $\chi_{\parallel c}/\chi_{\perp c}$ will be $3/(1 + 2\cos^2 \beta)$, where β is defined in Fig. 14. Therefore in case of a deviation from the 120° structure as expected for $RbVI_3$ the ratio $\chi_{\parallel c}/\chi_{\perp c}$ will be smaller than 2, depending on the ratio J_1/J_2.

Because of the paramagnetic contamination of $RbVI_3$ and $CsVI_3$ the ratio $\chi_{\parallel c}/\chi_{\perp c}$ cannot be determined. An estimation, made using a correction for a paramagnetic impurity, yields 1.8 for $CsVI_3$ and 1.3 for $RbVI_3$. In contradiction to $\chi_{\parallel c}/\chi_{\perp c}$ the exact value of $\chi_{\parallel c} - \chi_{\perp c}$ is known and this value is higher for $CsVI_3$ than for $RbVI_3$, although the averaged susceptibilities are about the same. $\chi_{\parallel c} - \chi_{\perp c}$ and the estimation of $\chi_{\parallel c}/\chi_{\perp c}$ suggest a deviation from the 120° structure for $RbVI_3$.

Although the magnetic measurements are hampered by contamination of the samples, they are in good agreement with the neutron powder diffraction results.

Acknowledgments

The author wishes to thank Dr R. A. G. de Graaff and Dr D. J. W. IJdo for the critical reading of the manuscript and Mr J. Strang of the Energiconderzoek Centrum Nederland for the performance of the neutron diffraction experiments.

References

1. H. J. SEIFERT AND K. H. KISCHKA, *Termochim. Acta* **27**, 85 (1978).
2. H. W. ZANDBERGEN, *J. Solid State Chem.* **37**, 189 (1981).
3. H. W. ZANDBERGEN, G. C. VERSCHOOR, AND D. J. W. IJDO, *Acta Crystallogr. Sect. B* **35**, 1425 (1979).

4. M. NIEL, C. CROS, M. POUCHARD, AND J. P. CHAMINADE, *J. Solid State Chem.* **20,** 1 (1977).
5. TING-I LI, G. D. STUCKY, AND G. L. MCPHERSON, *Acta Crystallogr. Sect. B* **29,** 1330 (1973).
6. J. W. WEENK, Thesis, Utrecht (1976).
7. T. SMITH AND S. A. FRIEDBERG, *Phys. Rev.* **176,** 660 (1968).
8. R. COLTON AND J. H. CANTERFORD, "Halides of the First Row Transition Metals," Wiley–Interscience, New York (1969).
9. H. T. WITTEVEEN, Thesis, Leiden (1973).
10. H. M. RIETVELD, *J. Appl. Crystallogr.* **2,** 65 (1969).
11. G. E. BACON, Compilation (1977).
12. R. E. WATSON AND A. J. FREEMAN, *Acta Crystallogr.* **14,** 27 (1961).
13. H. W. ZANDBERGEN, *J. Solid State Chem.* **35,** 367 (1980).
14. R. W. G. WYCKOFF, "Crystal Structures," 2nd ed., Vol. I, p. 269; Vol. III, pp. 341, 475, Interscience, New York (1964).
15. R. D. SHANNON AND C. T. PREWITT, *Acta Crystallogr. Sect. B* **25,** 925 (1969).
16. D. VISSER, G. C. VERSCHOOR, AND D. J. W. IJDO, *Acta Crystallogr. B* **36,** 28 (1980).
17. "International Tables for X-Ray Crystallography," Vol. II, p. 241, Kinoch Press, Birmingham (1959).